

DiracDiffusion: Denoising and Incremental Reconstruction with Assured Data-Consistency

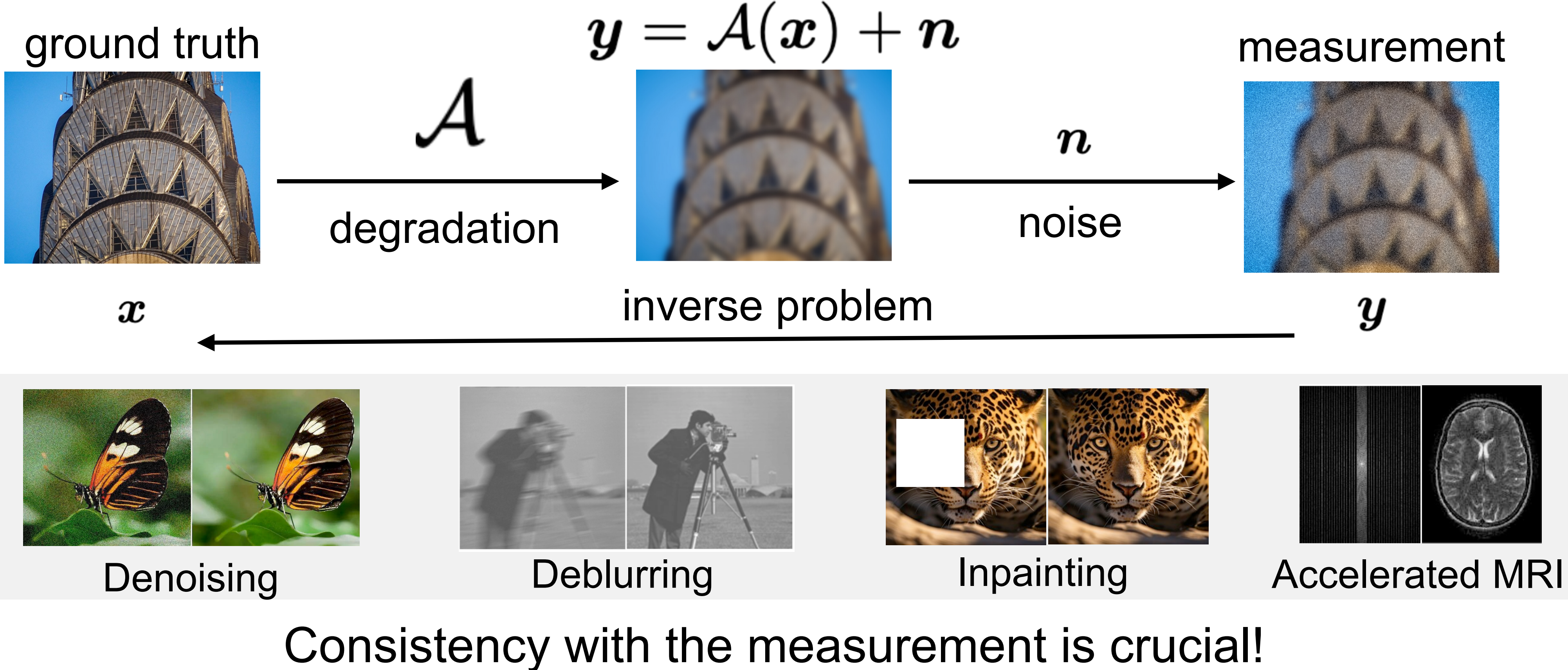
Zalan Fabian, Berk Tinaz, Mahdi Soltanolkotabi



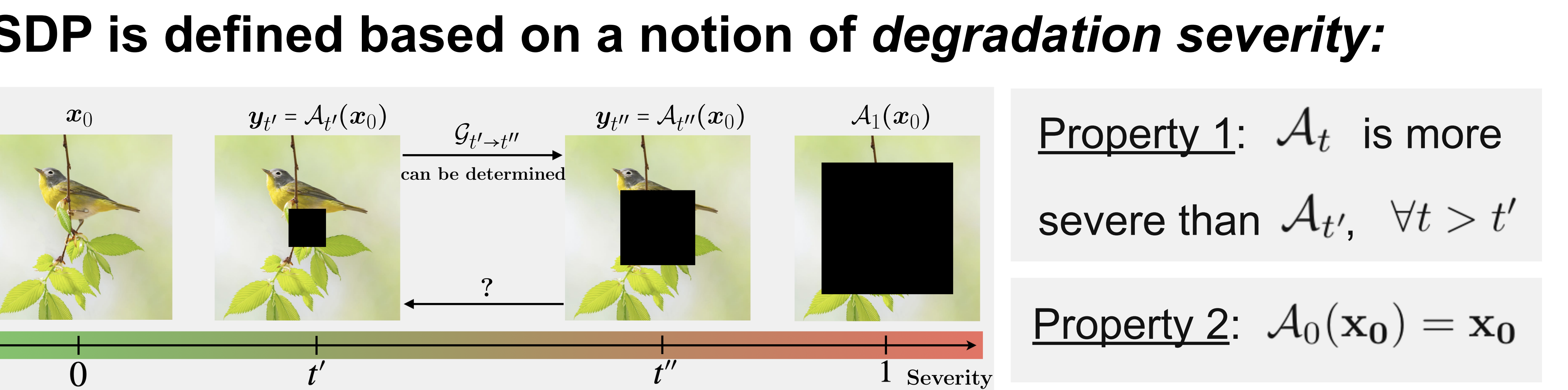
Paper

Code

Inverse problems

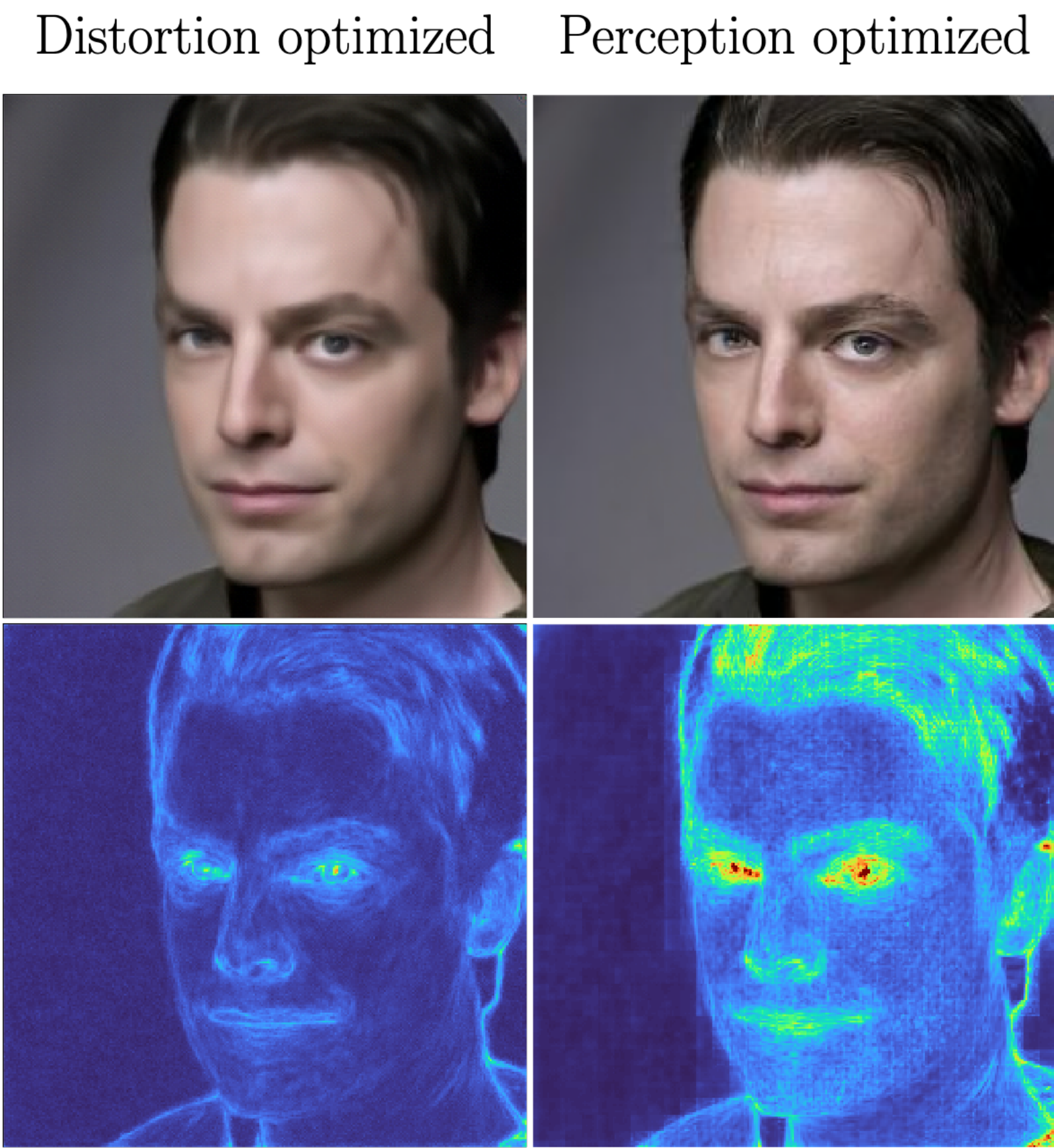


Degradation severity

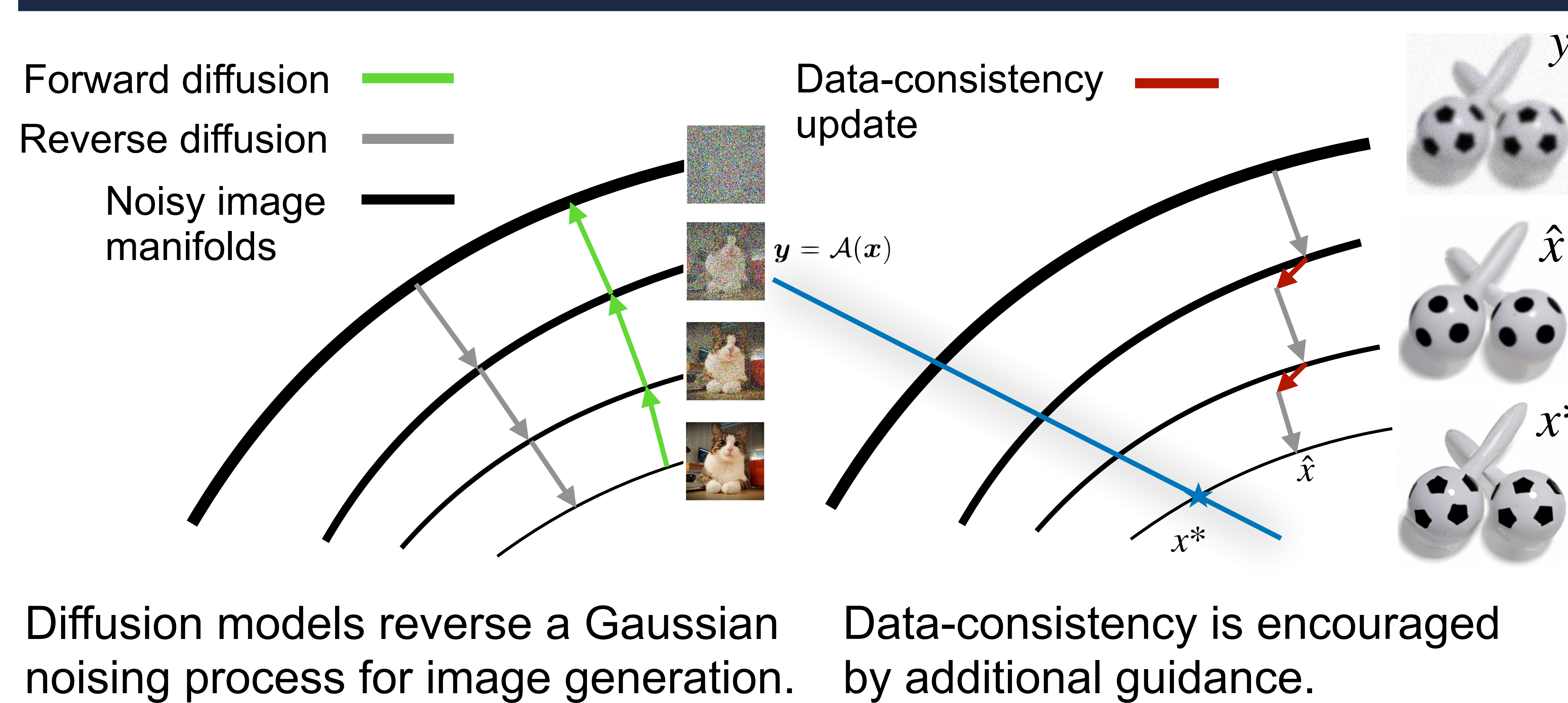


Perception-distortion trade-off

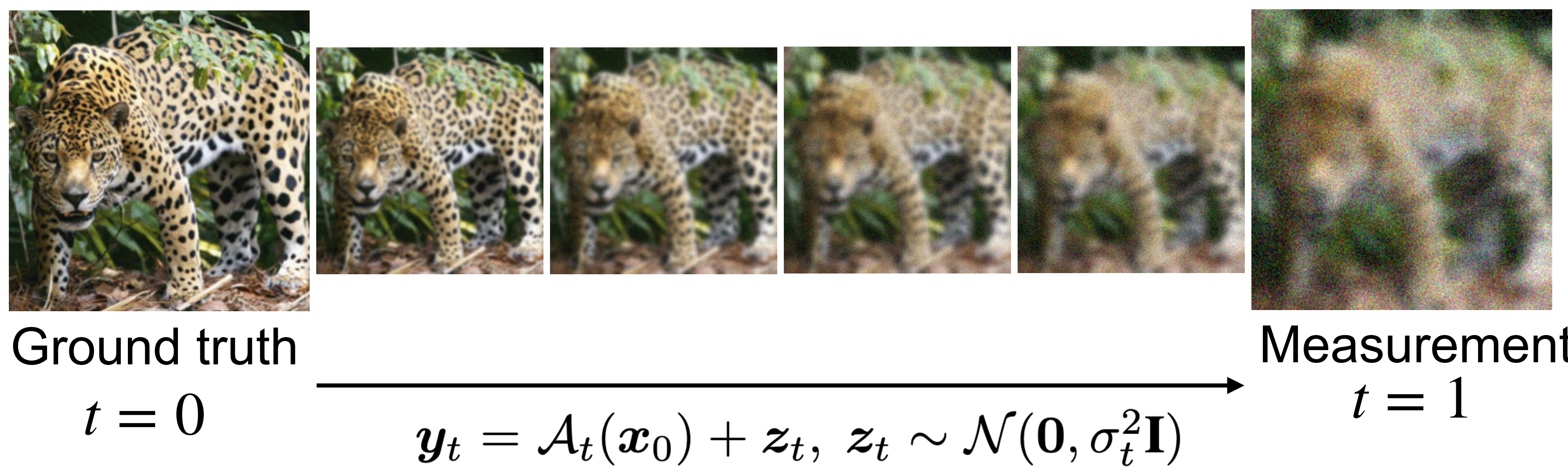
Perceptual image quality (LPIPS, FID) is fundamentally at odds with distortion (PSNR, SSIM). We control the trade-off via **early-stopping** the reverse process.



Diffusion solvers



Stochastic Degradation Process (SDP)

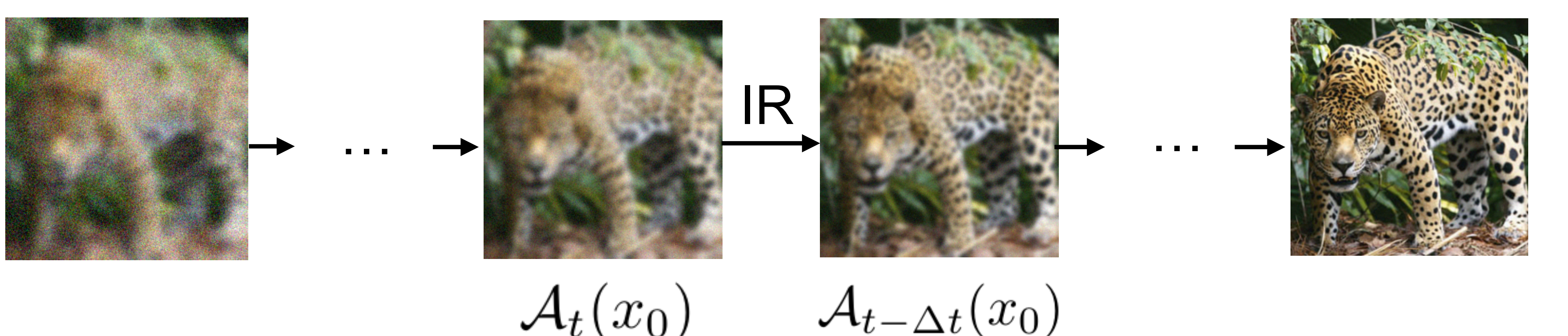


Reversing the SDP

$$\text{d}y_t = \dot{\mathcal{A}}_t(x_0)dt + \sqrt{\frac{d}{dt}\sigma_t^2}dw \xrightarrow{\text{reverse}} \xrightarrow{\text{discretize}}$$

$$y_{t-\Delta t} = y_t + \underbrace{\mathcal{A}_{t-\Delta t}(x_0) - \mathcal{A}_t(x_0)}_{\text{incremental reconstruction}} - \underbrace{(\sigma_{t-\Delta t}^2 - \sigma_t^2)\nabla_{y_t} \log q_t(y_t) + \sqrt{\sigma_t^2 - \sigma_{t-\Delta t}^2}z}_{\text{denoising}}$$

We learn to iteratively reverse small steps of degradation, which we call **incremental reconstruction** (IR).



Incremental Reconstruction Loss (IRL)

$$\mathcal{L}_{IR}(\theta) = \mathbb{E}_{t,(x_0,y_t)} [\|\mathcal{A}_{t-\Delta t}(\Phi_\theta(y_t, t)) - \mathcal{A}_{t-\Delta t}(x_0)\|^2]$$

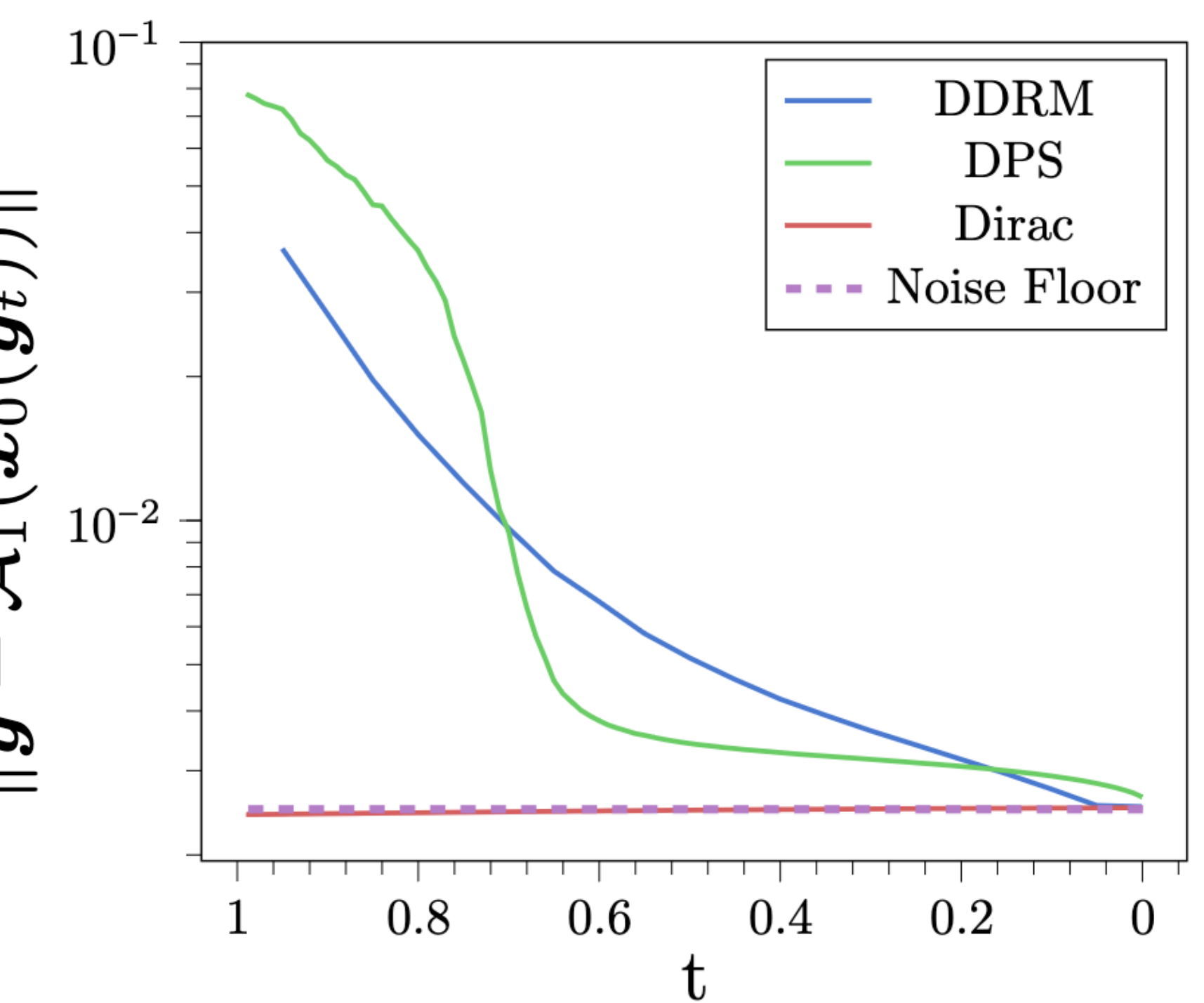
Given a degraded image with severity t , we predict a slightly less severe ($t - \Delta t$) degradation of the clean image.

Theoretical insights

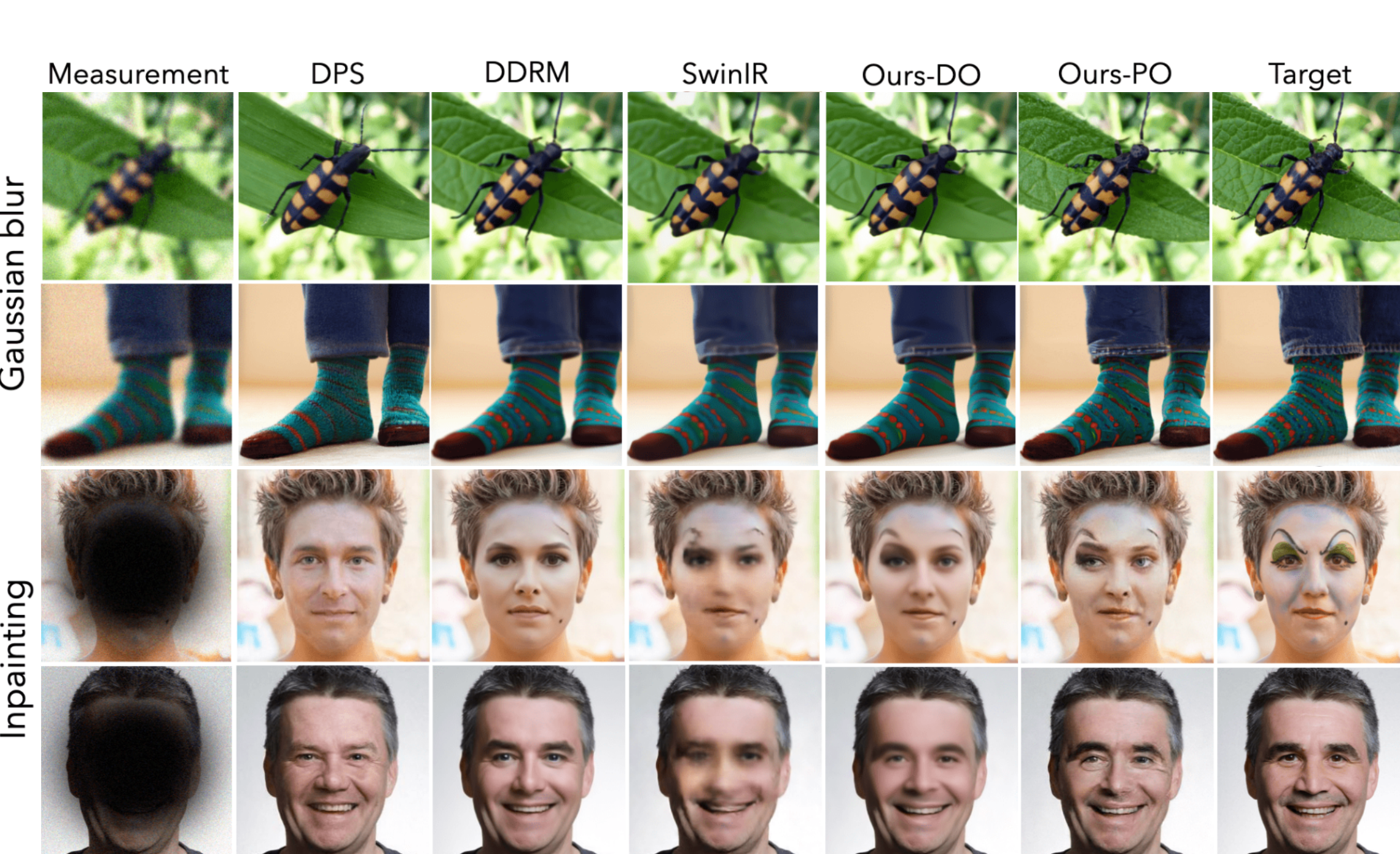
- Upper-bound on IR error depends on **degradation smoothness** (Theorem 3.4).
- Minimizing IRL enables learning **both** incremental reconstruction and denoising (Proposition A.6).
- Running **[UPDATE]** ensures **data-consistency** in every reverse diffusion step (Theorem 3.6).

Results

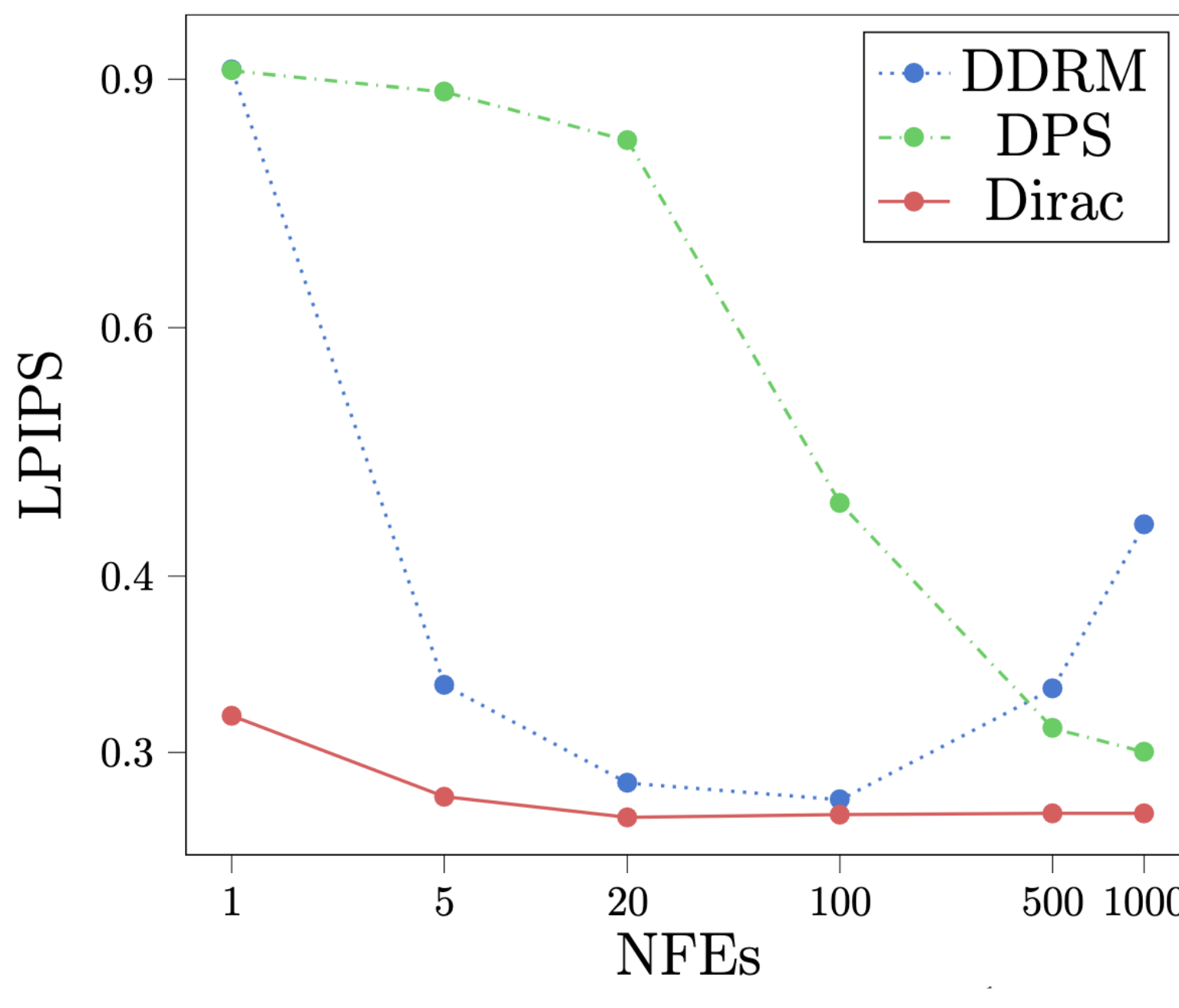
Data-consistency



Excellent reconstruction quality



Fast sampling



Method	Deblurring			Inpainting		
	PSNR(↑)	SSIM(↑)	LPIPS(↓)	PSNR(↑)	SSIM(↑)	LPIPS(↓)
Dirac-PO (ours)	26.67	0.7418	0.2716	53.36	0.7595	0.2611
Dirac-DO (ours)	28.47	0.8054	0.2972	69.15	26.98	0.8435
DPS (Chung et al., 2022a)	25.56	0.6878	0.3008	65.68	0.7238	0.2899
DDRM (Kumar et al., 2022a)	27.21	0.7671	0.2849	65.84	0.7362	0.2313
SwinIR (Liang et al., 2021)	28.53	0.8070	0.2848	72.93	0.7441	0.2934
PnP-ADMM (Chan et al., 2016)	27.02	0.7396	0.2973	74.17	0.7227	0.6035
ADMM-TV	26.03	0.7323	0.4126	89.93	11.73	0.5618

Method	Deblurring			Inpainting		
	PSNR(↑)	SSIM(↑)	LPIPS(↓)	PSNR(↑)	SSIM(↑)	LPIPS(↓)
Dirac-PO (ours)	24.68	0.6582	0.3302	53.99	0.8087	0.2079
Dirac-DO (ours)	25.76	0.7088	0.3705	63.23	0.8958	0.1766
DPS (Chung et al., 2022a)	21.51	0.5163	0.4235	52.60	0.7111	0.3825
DDRM (Kumar et al., 2022a)	24.53	0.6676	0.3917	61.06	0.7592	0.2138
SwinIR (Liang et al., 2021)	25.07	0.6801	0.4159	84.80	0.8490	0.2161
PnP-ADMM (Chan et al., 2016)	25.02	0.6722	0.4565	98.72	18.14	0.7901
ADMM-TV	24.31	0.6441	0.4578	88.26	17.60	0.7229

Table 1. Experimental results on the FFHQ (top) and ImageNet (bottom) test splits.